International Journal of Nanomedicine

Dovepress
open access to scientific and medical research

Open Access Full Text Article

ORIGINAL RESEARCH

Engineered Exosomes Containing microRNA-29b-2 and Targeting the Somatostatin Receptor Reduce Presenilin 1 Expression and Decrease the β-Amyloid Accumulation in the Brains of Mice with Alzheimer's Disease

En-Yi Lin[1,2], Shao-Xi Hsu[1], Bing-Hua Wu[1], Yu-Chen Deng[1,3], Wei Wuli[1], Yuan-Sheng Li[3], Jui-Hao Lee[3], Shinn-Zong Lin[2,4], Horng-Jyh Harn[2,5], Tzyy-Wen Chiou[1]

[1]Department of Life Science and Graduate Institute of Biotechnology, National Dong Hwa University, Hualien, Taiwan; [2]Bioinnovation Center, Buddhist Tzu Chi Medical Foundation, Hualien, Taiwan; [3]Everfront Biotech Inc, Taipei, Taiwan; [4]Department of Neurosurgery, Hualien Tzu Chi Hospital, Hualien, Taiwan; [5]Department of Pathology, Hualien Tzu Chi Hospital, Hualien, Taiwan

Correspondence: Tzyy-Wen Chiou, Department of Life Science, National Dong Hwa University, No. 1, Sec. 2, Da Hsueh Road, Shou-Feng, Hualien, Taiwan, Tel +886-3-890-3638, Email twchiou@gms.ndhu.edu.tw; Horng-Jyh Harn, Department of Pathology, Hualien Tzu Chi Hospital, Hualien, Taiwan, Tel +886-3-856-1825, Email arthewduke@gmail.com

Purpose: Exosomes are membrane vesicles secreted by various cells and play a crucial role in intercellular communication. They can be excellent delivery vehicles for oligonucleotide drugs, such as microRNAs, due to their high biocompatibility. MicroRNAs have been shown to be more stable when incorporated into exosomes; however, the lack of targeting and immune evasion is still the obstacle to the use of these microRNA-containing nanocarriers in clinical settings. Our goal was to produce functional exosomes loaded with target ligands, immune evasion ligand, and oligonucleotide drug through genetic engineering in order to achieve more precise medical effects.

Methods: To address the problem, we designed engineered exosomes with exogenous cholecystokinin (CCK) or somatostatin (SST) as the targeting ligand to direct the exosomes to the brain, as well as transduced CD47 proteins to reduce the elimination or phagocytosis of the targeted exosomes. MicroRNA-29b-2 was the tested oligonucleotide drug for delivery because our previous research showed that this type of microRNA was capable of reducing presenilin 1 (PSEN1) gene expression and decreasing the β-amyloid accumulation for Alzheimer's disease (AD) in vitro and in vivo.

Results: The engineered exosomes, containing miR29b-2 and expressing SST and CD47, were produced by gene-modified dendritic cells and used in the subsequent experiments. In comparison with CD47-CCK exosomes, CD47-SST exosomes showed a more significant increase in delivery efficiency. In addition, CD47-SST exosomes led to a higher delivery level of exosomes to the brains of nude mice when administered intravenously. Moreover, it was found that the miR29b-2-loaded CD47-SST exosomes could effectively reduce PSEN1 in translational levels, which resulted in an inhibition of beta-amyloid oligomers production both in the cell model and in the 3xTg-AD animal model.

Conclusion: Our results demonstrated the feasibility of the designed engineered exosomes. The application of this exosomal nanocarrier platform can be extended to the delivery of other oligonucleotide drugs to specific tissues for the treatment of diseases while evading the immune system.

Keywords: oligonucleotide drug, functional nanocarriers, hippocampus, SH-SY5Y, 3xTG-AD

Introduction

In accordance with a report issued by the World Health Organization,[1] there are 55 million people worldwide who suffer from dementia, of which 60–70% have AD. In spite of the growing number of patients with AD, there is still no effective drug for its

Received: 23 January 2024
Accepted: 26 April 2024
Published: 29 May 2024

clinical treatment. Therefore, it is urgent to develop new therapeutic strategies that can effectively delay the progression of the disease, alleviate the symptoms, and enhance cognitive function. Our previous study demonstrated that by increasing miRNA-29b-2-5p expression, the PSEN-1 gene could be targeted and inhibited, thus reducing the activity of γ-secretase and reducing amyloid production.[2] In light of this, we consider miRNA-29b-2-5p has the potential to be developed into a new anti-Alzheimer's oligonucleotide drug.

There are two types of AD: early-onset AD (also known as familial AD) and late-onset AD (also known as sporadic AD).[3] In general, early-onset AD accounts for only 5% of all cases of AD. Its cause, however, is primarily related to gene mutations. An abnormal presenilin 1 (PSEN1) is produced by the presenilin 1 gene mutation present on the 14th pair of chromosomes. As the most common AD gene mutation, PSEN1 accounts for roughly 50% of early-onset disease-causing genes.[4,5] Mutations in PSEN1 that carry only a single allele increase the risk of developing late-onset AD.[6] PSEN1 is one of the components of γ-secretase. One of the strategies for developing drugs to treat AD is to inhibit the cleavage of γ-secretase and reduce the production of amyloid.

Current studies on oligonucleotide drugs include antisense oligonucleotide (ASO), small interfering RNA (siRNA), microRNA (miRNA), and aptamers.[7] MiRNA is a non-coding RNA molecule consisting of 21–25 nucleotides. In organisms, miRNA can affect the transcription of message RNA (mRNA). The process plays an important role in regulating cellular transcription, cellular development, and disease progression.[8,9] There are specific miRNAs that are strongly associated with AD. As of now, it is known that there are around 14 miRNAs that are increased in the brains of patients with AD, and about 36 that are decreased.[10] In addition, multiple miRNAs have been demonstrated to be down-regulated in the blood and cerebrospinal fluid of patients with AD.[11,12] The development of oligonucleotide drugs will be one of the most important trends in drug development in the future. Based on our previous studies, we have determined that the mechanism of action of n-butylidenephthalide (BP), a small molecule drug used to treat AD, is to modulate PSEN-1 and to reduce the production of amyloid protein through miRNA-29b-2-5p. Therefore, miRNA-29b-2-5p is considered a novel oligonucleotide-targeted drug.[2] In this study, we chose miRNA-29b-2, the precursor miRNA of miRNA-29b-2-5p, as the target oligonucleotide.

Liposomes encapsulate small molecules efficiently, and they have a simple composition, which makes them an attractive method for encapsulating small molecules.[13] In comparison to liposomes, exosomes possess low immunogenicity, high biocompatibility, and flexible targeting, making them ideal delivery vehicles and nanocarriers for oligonucleotide drugs (such as microRNA). The exosome carries mRNA, miRNA, protein, or metabolites for varying distances between cells. MiRNA concentrations in exosomes are also higher than those in cells.[14] Previous investigation has shown that exosomes could be used as a platform for the delivery of nucleic acids.[15] Since exosome-encapsulated miRNAs were more stable than naked miRNA, they could move in the body without being easily hydrolyzed by hydrolytic enzymes. After the exosome-encapsulated miRNAs entered the receiving cells, they were still able to perform its functions.[16]

It is known that specific miRNAs in exosomes can be increased by overexpressing them in the secreting cells. This indicates that using cell factories to produce exosomes containing specific miRNAs and using them as drug delivery vehicles has great potential.[17–19] Exosomes released by immature dendritic cells (DC) contain substances that are rich in self-antigens and anti-inflammatory factors, and they may promote or induce immune tolerance. Since DC-derived exosomes contain only a small amount of MHC II and CD86, they do not stimulate the immune system and have immunosuppressive properties.[20,21] Immature DC-derived exosomes have generally been shown to promote the survival of allotransplants by secreting IL-10, an anti-inflammatory cytokine that inhibits T cell proliferation.[22] Exosomes derived from immature DCs are rich in autologous antigens and anti-inflammatory factors, and have low levels of MHC II and costimulatory CD86+ molecules, so they are unable to initiate immune responses and exhibit immunosuppressive properties.[23]

To reduce the side effects caused by off-target effects and increase the effectiveness of oligonucleotide drugs, a more precise method is required. Generally, after being administered systemically, RNA accumulates in the kidneys and is excreted by the urine.[24] On the other hand, the hippocampus is responsible for the memory center of the human brain. In an animal model of AD, it was found that β-amyloid could accumulate in the hippocampus.[25] The addition of amyloid to the hippocampus of normal rats can also lead to the loss of working memory.[26] β-amyloid accumulation in the hippocampus has been demonstrated to be one of the major factors driving the progression of AD. Due to this fact, this study uses a target design focused on targeting the hippocampal region. Because of the presence of specific receptors

in the hippocampal region of the brain for cholecystokinin (CCK)[27] and somatostatin (SST),[28,29] these two ligands were selected as the target ligands in this study.

In order to target the hippocampus, CCK or SST are engineered for surface expression on exosomes with a hippocampus-targeting mechanism. Based on the fact that CD47 is expressed on the membrane of exosomes,[30] the target gene could be designed to be expressed at the surface of exosomes.[31] Using the exosome carrier, the oligonucleotide drug (miRNA-29b-2) is targeted to the hippocampus memory area of the brain for the treatment of AD.

In addition, Integrin-associated proteins (IAPs) are surface immunoglobulin molecules that interact with signal regulatory proteins alphas (SIRPs) and send the "Don't eat me" signal. Inhibition of the CD47-SIRPα signaling pathway leads to phagocytosis of macrophages and enhances the adaptive immune response.[32] Exosomes produced by T cells, such as Jurkat cells and human foreskin fibroblasts, carry CD47 ligands on their surfaces and can prolong their half-life in the blood.[33,34] This property makes exosomes with CD47 present in the membrane an attractive candidate for use as a drug carrier. Therefore, genes can be transferred to various cells that produce exosomes during genetic engineering, leading to the production of exosomes expressing CD47 ligands.

Due to the short half-life of oligonucleotide drugs, difficulty in entering cells, and inability to reach targets by general administration, this study developed miRNAs that could stably transport and silence disease-causing genes, along with an exosome-based platform for targeting the hippocampus. We performed a series of experiments to analyze the physical properties and biological indicators of engineered exosomes. In addition, both in vitro model and mouse models of AD were used to assess and verify the efficacy of this targeted engineered exosomes.

Materials and Methods

Generation of Lentiviruses Carrying miRNA 29b-2, Immune Evasion and Target Genes (CD47-CCK or CD47-SST)

The hsa-mir-29b-2 gene was constructed into a lenti-vector pMIRNA1 (System Bioscience, California, USA) (carrying a green fluorescent protein and an ampicillin resistance genes). The target gene (cholecystokinin or somatostatin) and the immune checkpoint gene CD47 were simultaneously incorporated into pLVX-IRES-tdTomato (631,238, Takara, California, USA) (carrying an orange fluorescent protein and an ampicillin resistance gene). Construction of clones expressed gene fragments of CD47 (GenBank Reference Sequence: HQ585874.1) and CCK (NCBI Reference Sequence: NM_031161.4) or SST (GenBank Reference Sequence: BC010770.1) were amplified by PCR with insertion of EcoRI at the 5' end and BamHI at the 3' end. The primers used were show as Table 1 and Figure 1A. The DNA plasmids were produced using DH5α (18,263,012, Thermo Fisher Scientific, Massachusetts, USA). To determine the genomic accuracy of the plasmids, colony polymerase chain reaction (PCR), restriction enzymes, and DNA sequencing were used. HEK293T (CRL-3216, ATCC, Georgia, USA) was used for lentiviral packaging and production of miRNA 29b-2, target

Table 1 The Primer Used in the Construction of Plasmids

Primer Name	Sequence(5' to 3')
Vector_F: 35 nt	GGA TCC CGC CCC TCT CCC TCC CCC CCC CCT AAC GT
Vector_R: 35 nt	CTT GTC ATC GTC GTC CTT GTA GTC CAT GGT GGC GA
CD47_F: 35nt	GAC GAC GAT GAC AAG ATG TGG CCC TTG GCG GCG GC
CD47_R1: 25nt	CCT ATT CCT AGG AGG TTG GAT AGT C
CCK_F1: 35 nt	CCT CCT AGG AAT AGG ATG AAG AGC GGC GTA TGT CT
CCK_R: 35 nt	AGA GGG GCG GGA TCC TTA AGA ACG GAC ATG CGG CC
SST_F1: 35 nt	CCT CCT AGG AAT AGG ATG CTG TCC TGC CGT CTC CA
SST_R: 35 nt	AGA GGG GCG GGA TCC CTA ACA GGA TGT GAA TGT CT

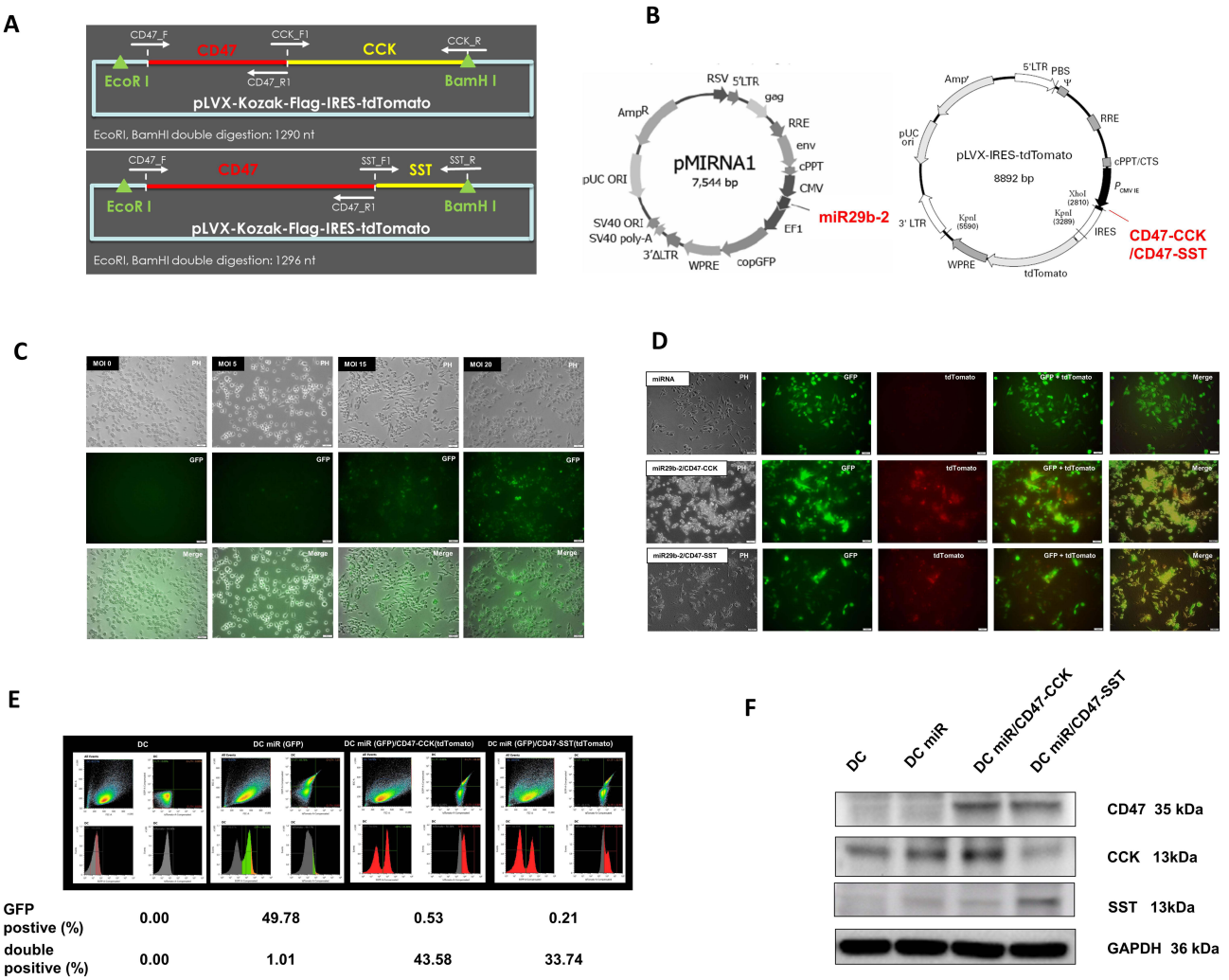

Figure 1 Dendritic cells transfected with miR-29b-2 and CD47-SST lentiviral vectors. (**A**) Construction design for CD47-CCK and CD47-SST plasmids. (**B**) Designs for two different constructs. (**C**) pMIRNA1 lenti-vector (green fluorescent) carrying miR29b-2 transfected dendritic cells. (Scale bar represents 50 μm) (**D**) pLVX-IRES-tdTomato lenti-vectors (red fluorescence) were used to transfect the miR29b-2-DC with target gene CCK or SST, and immune immunity gene CD47. (Scale bar represents 50 μm) (**E**) The sorting of cells. DC cell sorting with a double positive ratio. (**F**) Detection of target gene (CCK or SST) and immune immunity gene CD47 on Western blots.

genes (cholecystokinin and somatostatin), and CD47. Subsequently, 4–5×10^6 HEK293T cells were cultured in a 10 cm dish, according to standard conditions. After cells had grown to a certain number, plasmid DNA (miRNA 29b-2, CD47, CCK and SST) carrying transfection gene and lentiviral vector DNA with transfection reagents (Lenti-X Packaging Single Shots (VSV-G), 631,275, Takara, California, USA) were added to the cell culture. After adding the lentiviral supernatant, a collection of the lentiviral supernatant was taken approximately 24 to 48 hours later. The supernatant was then concentrated with a virus concentrate solution (Lenti-X Concentrator, 63,123, Takara, California, USA) and quantified with a p24 rapid titer kit (Lenti-X p24 Rapid Titer Kit, 632,200, Takara, California, USA).

Transduction of Lentivirus into Dendritic Cells and Cell Sorting

The TransDux (TransDux virus transduction reagent (200x), LV850A-1, System Bioscience, California, USA) reagent was diluted in DC culture medium to a final concentration of 1x before it was added to the DCs. Transducing dendritic cells was accomplished by adding diluted 1x TransDux reagent with lentivirus containing miRNA 29b-2 and immune evasion gene with the target gene (CD47-CCK or CD47-SST). The number of cells and the virus to cell ratio (MOI) was determined before this step had been undertaken. Once the viral genome was integrated into the host genome, it became

part of it. Subsequently, the cells were sorted and amplification was performed. The SH800 Cell Sorter (Sony Biotechnology, California, USA) was used to collect isolated dendritic cells expressing fluorescent GFP (with pMIRNA1-miRNA 29b-2) and dendritic cells expressing GFP and tdTomato (with pMIRNA1-miRNA 29b-2). The supernatants were collected separately after the cells had been amplified, followed by the extraction of exosomes.

Evaluation of CD47, CCK and SST Expression in Cells Infected with Lentiviruses

Analysis of the protein content of lentivirus after transmission into DC cells was conducted by Western blot experiments in order to verify that the lentivirus plasmid was introduced into the cells.

The following products of primary antibody were utilized: anti-CD47(GTX132762, GeneTex, California, USA), anti-CCK (SAB2100357, Sigma-Aldrich, Massachusetts, USA) anti-SST (GTX133119, GeneTex, California, USA), and anti-GAPDH (MAB374, Sigma-Aldrich, Massachusetts, USA). DC cells that had been transfected were lysed in RIPA buffer (150 mM sodium chloride, 50 mM Tris, 1% NP-40, 0.5% sodium deoxycholate, 0.1% sodium dodecyl sulfate), and their protein concentration was assessed by BCA. LDS degeneration buffer (Bio-Red) in an equal volume with 2-Mercaptoethanol was used. SDS-PAGE gels of 12% BIS-TRIS base were used to electrophoretically separate the different molecular weight proteins. After this procedure, the protein transferred to the PVDF membrane. Following that, the membrane was blocked with either 5% milk/PBST (containing 0.05% Tween-20) or 5% bovine serum albumin (BSA)/PBST. The primary antibodies were diluted 1-to-1000 in 2% BSA/PBST and added to PVDF membranes in a solution of 2% BSA/PBST. At 4°C, the membranes were soaked and shaken overnight. PVDF membranes were washed with PBST and added to 2% BSA/PBST with HRP-conjugated secondary antibodies, then shaken for one hour at room temperature. Horseradish peroxidase (HRP) and chromogenic substrates were used to bind the secondary antibody, followed by imaging using a gel imaging system (iBright Imaging Systems, Thermo Fisher Scientific, Massachusetts, USA) to capture the images. In order to calculate the relative signal of the target antibody compared with the standardization of the internal control GAPDH, IMAGE J was used to calculate the densities of the bands and make comparisons.

The Production and Purification of Exosomes

Dendritic cells were cultured following different lenti-vector transductions in multilayer T-flasks (353,144, Falcon & 353,143, Falcon). Once the cells had reached 80% fullness, serum-free and phenol red-free media were replaced. After 72 hours of incubation, the supernatant was collected and frozen at −20°C. After the supernatant accumulating to a certain volume, the process of exosome purification was carried out. To concentrate the protein larger than 100 kDa, a centrifuge tube with a molecular weight cut-off of 100 kDa (Amicon® Ultra-15 Centrifugal Filter Unit, UFC910008, Millipore) was used, followed by separating the exosomes from the concentrate and purifying the exosomes using polymer precipitation (ExoQuick-TC, EXOTC,50A-1, System Bioscience, California, USA). The pellet was then redissolved in particle-free PBS (resolution volume set at 1/1000 of the original volume). The exosomes were stored at −80°C once they have been aliquoted, and they should not be frozen and thawed repeatedly.

Characterization of Engineered Exosomes on a Physical, Chemical, and Functional Level

The Analysis of miRNAs in Engineered Exosomes

A quantitative polymerase chain reaction (qPCR) was performed in order to confirm the amount of miRNA-29b-2-5p in the exosomes obtained. The exosomes were isolated and purified using Invitrogen Total Exosome RNA & Protein Isolation Kit (4,478,545, Thermo Fisher Scientific, Massachusetts, USA). Total RNA was then measured for absorbance (OD260/280 nm). To reverse transcription cDNA, Mir-X miRNA First Strand Synthesis Kit (638,315, Takara, California, USA) was used. A real-time polymerase chain reaction was then performed with the SYBR green master mix kit that is included in the TB Green® Premix Ex Taq™ (RR420L, Takara, California, USA). The polymerase chain reaction was conducted using an ABI QuantStudio 3 Real-Time PCR System. CTGGTTTCACATGGTGGCTTAG is the primer sequence for miR-29b-2-5p.

Measurement of Exosome Particle Size and Concentration

With the Malvern Panalytical NanoSight NS300 and Malvern Panalytical's NanoParticle Tracking Analysis (NTA), nanoscale particle sizes, counts, and concentrations were determined. Exosome stocks were diluted 10,000 times with particle-free PBS before being injected into the instrument using a syringe at a constant flow rate. The flow rate (syringe pump speed) was 100 and the detection threshold was 5. Each sample was collected three times for 60 seconds in order to determine its average value. The number, strength, and size of exosomes were calculated based on the flow rate and Brownian motion of nanoparticles. The concentration was also determined based on the injection volume and number of particles.[35]

Zeta Potential Analysis of Exosomes

Zeta potential is crucial to understanding flocculation and sedimentation, as well as the stability of exosomes. To determine the stability of particle-particle interactions and the tendency of particles to aggregate, the Malvern Zetasizer Nano S was used to measure the zeta potential. The zeta potential of exosomes is typically negative and is affected by the concentration of ions and the pH of the environment.[36] The exosomes from various groups (DC exo, DC miR exo, DC miR29b/CD47-CCK exo, miR29b/CD47-SST exo) were dispersed 1×10^8 / mL in physiological saline, and then were added to disposable folded capillary cells (DTS1070, Malvern Panalytical, Malvern, UK). The RI value was set at 1.56 and water was used as the dispersant. Smoluchowski's equation was used to calculate the diffusion equation. There were 20 runs in each test, resulting in a total of three measurements with a 20 second delay between each measurement.

Analysis of Engineered Exosomes Expressing CD47, CCK, SST, and Exosome Protein

The protein expression in exosomes produced by DC cells was examined after the lentivirus had been transduced into the cells. Among the primary antibodies used are anti-CD47 (GTX132762, GeneTex, California, USA), anti-CCK (SAB2100357, Sigma-Aldrich, Massachusetts, USA), anti-SST (GTX133119, GeneTex, California, USA), anti-CD81 (GTX135297, GeneTex, California, USA), and anti-HSP70 (SC-32239, Santa Cruz Biotechnology, Texas, USA). As the exosome protein lysate decomposes, it was separated on a gel electrophoresis based on its molecular weight. Afterwards, the gels were transferred to the membrane. Protein expression was demonstrated by binding the protein-specific antibody to the membrane, using horseradish peroxidase (HRP) with chromogenic substrates, and imaging the gel (iBright Imaging Systems, Thermo Fisher Scientific, Massachusetts, USA). The total protein identified by Ponceau S (A40000279, Thermo Fisher Scientific, Massachusetts, USA) in exosomes was used as an internal control.

Transmission Electron Microscopy (TEM) Examination of Exosome Morphology

The exosome droplets were deposited onto carbon-coated grids and 2% uranyl acetate was applied for negative staining. Before examination, grids were air-dried. The examination was conducted at a voltage of 80 kV using a Hitachi H-7500 transmission electron microscope (Hitachi, Tokyo, Japan). Recorded images were obtained using an AMT NanoSprint12: 12 Megapixel sCMOS TEM camera (Advanced Microscopy Techniques, Woburn, MA).

A Cellular Model of AD Cell Model -SH-SY5Y

As a cell model for AD, differentiated and induced human neuroblastoma SH-SY5Y (CRL-2266, ATCC, Georgia, USA) cells were used. The medium was supplemented with 10% Fetal Bovine Serum (16,000,044, Gibco, Thermo Fisher Scientific, Massachusetts, USA) and 1% Penicillin-Streptomycin solution (SV30010, Hyclone, Cytiva, Washington, D.C., USA) in DMEM/F12 (12,634,010, Gibco, Thermo Fisher Scientific, Massachusetts, USA). The cells were incubated at 37°C with 5% CO_2. When the cells had grown to 80% full in T-Flask, 10^5 cells were seeded per well in a 6-well plate precoated with 50 μg/mL poly-D-lysine (354,210, Scientific Laboratory Supplies, England, UK).

For cell differentiation, the medium was replaced with 1% low-serum DMEM/F12 with 1% FBS, 1% P/S, and 10 μM retinoic acid (RA) (R2625, Sigma-Aldrich, Massachusetts, USA) culture medium and cultured for 72 hours. The old medium was replaced with new medium containing 50 ng/mL BDNF and incubating for 72 hours. In addition, cytotoxicity was further induced after SH-SY5Y cells had been differentiated with RA (10 μM) (R2625, Sigma-Aldrich, Massachusetts, USA) and 50 ng/mL BDNF (CYT-207, Prospec, Ness-Ziona, Israel) for 7 days. 20 μM

Aβ1-42 oligomer (HY-P1363, MedChemExpress, New Jersey, USA) and 10 μM Okadaic acid (OA) (495,604, Sigma-Aldrich, Massachusetts, USA) was then added for 24 hours to induce the expression of AD proteins in cells.[37]

Culture of Dendritic Cells DC2.4

The mouse cell DC2.4 (SCC142M, Merck, Darmstadt, Germany) were cultured in RPMI-1640 (CC110-0500, GeneDireX, Taipei, Taiwan) medium containing 10% FBS (16,000,044, Gibco, Thermo Fisher Scientific, Massachusetts, USA), 1X L-Glutamine, 1X non-essential amino acids (11,140,050, Gibco, Thermo Fisher Scientific, Massachusetts, USA), 1X HEPES buffer solution (15,630,080, Gibco, Thermo Fisher Scientific, Massachusetts, USA), 0.0054X β-Mercaptoethanol (ES-007-E, Merck, Darmstadt, Germany) and 100 ng/mL penicillin and streptomycin (11,548,876, Gibco, Thermo Fisher Scientific, Massachusetts, USA). The original RPMI-1640 medium with phenol red was replaced with a phenol red-free RPMI-1640 medium (CC111-0500, GeneDireX, Taipei, Taiwan) and serum-free medium prior to exosome harvesting.

Identification of Cell Target Receptors

To verify that CCK or SST ligands target specific CCK or SST receptors in cells, we first determined the amount of the target receptors in SH-SY5Y cells. The SH-SY5Y cells were harvested and incubated in a lysis buffer containing 150 mM sodium chloride, 50 mM Tris, 1% NP-40, 0.5% sodium deoxycholate, and 0.1% sodium dodecyl sulfate. BCA method was used to determine the total protein content. The amount of SSTR protein was evaluated using the Western blot method, as described above. Primary antibodies used were anti-CCKBR (SAB4503491, Sigma-Aldrich, Massachusetts, USA), anti-Somatostatin receptor 3 (GTX130114, GeneTex, California, USA), and anti-GAPDH (MAB374, Sigma-Aldrich, Massachusetts, USA).

Evaluation for the Cellular Uptake of Exosomes

To establish that CCK or SST ligands target specific CCK or SST receptors, an investigation of the cellular uptake of exosomes was undertaken. The cells derived from SH-SY5Y were cultured on four-well glass chamber slides (PEZGS0416, MiliporeSigma, Darmstadt, Germany) and treated with $3x10^8$/mL of different exosomes (DC exo, DC miR exo, DC miR29b/CD47-CCK exo, miR29b/CD47-SST exo). The exosomes from each group were first labeled with green fluorescent DiO (3,3'-Dioctadecyloxacarbocyanine perchlorate, 42,367, Sigma-Aldrich, Massachusetts, USA). Exosomes were labeled by adding 2μg/mL of DiO to $5x10^9$/mL of exosomes. Dio-exosomes were sonicated for ten minutes, put on ice for one hour, and then precipitated using ExoQuick-TC (50A-1, System Bioscience, California, USA). Following dissolution in particles-free PBS, the exosomes were quantified using the NanoSight NS300 (Malvern Panalytical, Worcestershire, UK).

Inhibition of Disease-Associated Proteins

An analysis of PSEN1 and Aβ oligomer 1–42 proteins expression in AD cell models was performed following exosome treatment. The cells were harvested and incubated in lysis buffer containing 150 mM sodium chloride, 50 mM Tris, 1% NP-40, 0.5% sodium deoxycholate, and 0.1% sodium dodecyl sulfate. The total protein content of the sample was determined by BCA analysis. Western blots were used to determine the amount of disease proteins in the samples. The primary antibodies used were anti-PSEN1 (GTX116016, GeneTex, California, USA), anti-Aβ oligomer 1–42 (AB5078P, Sigma-Aldrich, Massachusetts, USA), and anti-GAPDH (MAB374, Sigma-Aldrich, Massachusetts, USA).

In vivo Imaging System (IVIS) Analysis of Exosome Distribution

To understand the distribution of exosomes in animals, the following experiments were conducted. DiR (1,1-dioctadecyl-3,3,3,3-tetramethylindotricarbocyanine iodide, HY-D1048, MedChemExpress, New Jersey, USA) was further labeled with various groups of exosomes. A variety of DIR exosomes (DC exo, DC miR exo, miR29b/CD47-SST exo) of a dose of 2.5×10^{10} / 250 μL were injected into mice's tail veins. Approximately 24 hours later, three animals from each group were imaged by fluorescence. The experiments were conducted with nude mice (CANN.Cg-*Foxn1*^{nu}/CrlNarl) (National Laboratory Animal Center, Taipei, Taiwan) that make fluorescence distribution easier to observe. Exosomes were

monitored in vivo using the In Vivo Imaging System from Perkin Elmer (IVIS Spectrum, Connecticut, USA). For maximum sensitivity, the system utilizes a charge coupled device cooled to −90°C. A field of view was chosen based on the number of animals to be photographed, an exposure time of two seconds was set, and a light source with an excitation wavelength of 710 nm and an absorption wavelength of 760 nm was used to capture the images. The images were adjusted and analyzed in Living Image software. Since this experiment was conducted at the Animal Center of National Dong Hua University (NDHU), the experiment has been approved by the Institutional Animal Care and Use Committee (IACUC) of NDHU (IACUC NO.110003). The animals were fed ad libitum and kept in a light-dark cycle of 12 hours a day. The procedures for the care of animals are conducted in accordance with Taiwan's Animal Protection Law and the regulations of the Animal Care Committee of NDHU.

Analysis of Disease Proteins in Animal Tissues

To evaluate the therapeutic effect in animals, we used 8-month-old 3xTg-AD (The Jackson Laboratory, Sacramento, CA, USA) female mice for treatment, divided them into three groups including untreated (UT), DC exo-treated, and DC miR/CD47-SST-treated groups. A total of 2.5×10^{10} exosomes were injected into the tail vein. Three days later, the mice were sacrificed and their brains were cut longitudinally. Approximately half of these samples were detected by Western blot, while the other half were detected by Immunohistochemistry.

In order to determine whether the mouse cortex and hippocampus contained PSEN1 and Aβ oligomer 1–42 disease proteins by Western blot, the tissue was directly refrigerated after it had been sliced under pre-cooled PBS. The samples were then mechanically disrupted and lysed using RIPA buffer (150 mM NaCl, 50 mM Tris, 1% NP-40, 0.5% sodium deoxycholate, 0.1% sodium lauryl sulfate). The concentrations of protein were determined by BCA, followed by identification by Western blotting. Anti-Aβ1-42 (AB5078P, Sigma-Aldrich, Massachusetts, USA), and anti-GAPDH (MAB374, Sigma-Aldrich, Massachusetts, USA) were used as primary antibodies in the experiment. As this experiment was performed at the Animal Center of Tzu Chi University, the protocol has been approved by Hualien Tzu Chi Hospital (IACUC No.108–04). The mice of B6;129-Tg (APPSwe, tauP301L)1Lfa *Psen1*^{tm1Mpm}/Mmjax strain were also fed ad libitum and kept in a light-dark cycle of 12 hours a day. Animal care procedures are implemented in accordance with the Animal Protection Law in Taiwan and the Guide for the Care and Use of Laboratory Animals of Tzu Chi University.

Immunohistochemistry(IHC) for Detecting Disease Proteins and Exosome Proteins

The brains of mice were cut longitudinally for tissue sampling, and half of the samples were fixed in 10% formalin. The tissues were fixed, dehydrated, and embedded in paraffin wax. Tissue sections were cut from fixed tissue blocks using a microtome (RM2135, LEICA, Solms, Germany), with a thickness of 3 μm. The tissue slides were dewaxed, rehydrated, and antigen-retrieved (QD430-XAKE, BioGenex, California, USA) before 5% blocking of fetal bovine serum was added to prevent non-specific antibody binding. To bind the target antigen to the tissue, primary antibodies anti-Aβ1-42 (AB5078P, Sigma-Aldrich, Massachusetts, USA), anti-CD47 (GTX132762, GeneTex, California, USA), anti-SST (GTX133119, GeneTex, California, USA) or anti-CD63 (GTX132953, GeneTex, California, USA) were added. Once the unbound primary antibody has been removed, the secondary antibody that is specifically recognized for binding to the primary antibody was added. Afterward, the color was developed using DAB, counterstain was applied with hematoxylin, and the material was dehydrated before being mounted.

Silencing of SST Receptor 3 in SH-SY5Y Cells

A sequence of siRNA for SST receptor 3 was synthesized by the GeneDireX company (Taipei, Taiwan). This was a forward sequence of 5'-GGACAUGCUUCAUCCAUCATT-3' and a backward sequence of 5'-UGAUGGAUGAAGCAUGUCCTT-3'. The Lipofectamine 2000 was purchased from the Invitrogen Corporation (Massachusetts, USA). The siRNA was transfected into the SH-SY5Y cells. The cells were plated in 6-well plates, the medium in the plates was discarded after the cells had reached an appropriate density, and 1 mL of Opti-MEM (31,985,062, Gibco, Thermo Fisher Scientific, Massachusetts, USA) blank medium was added to starve the cells. The Lipofectamine 2000 and siRNA were mixed with 150 μL of Opti-MEM blank medium at 9 μL and 3 μg each, and then combined. Following mixing of the above two types of medium and standing the mixture at room temperature for five minutes, the mixture was added to starved cells. After 48 hours

of incubation at 37°C with 5% CO_2, the liquid in the plate was discarded and replaced with fresh complete medium. Studies were conducted later on the quantification of proteins and the uptake of these proteins by cells.

Statistical Analysis

The Student's *t*-test was used in this study to determine whether the experimental results are statistically significant. A *p*-value less than 0.05 was considered statistically significant. All data are presented as mean ± standard deviation.

Results

Establishment of a Cell Model That Produces Engineered Exosomes

To facilitate the production of exosomes containing specific gene expression, we initially transfected the target gene into dendritic cells using the lenti vector system (Figure 1B). A lentiviral vector containing miR29b-2 was transfected into dendritic cells using pMIRNA1 lenti-vector. The most appropriate transfection conditions were selected (MOI 15, 24 hours). The cells were then scaled up and cultured after transfection (Figure 1C). These dendritic cells were co-transfected with miR29b-2 using pLVX-IRES-tdTomato lenti-vectors (orange fluorescent) carrying the target gene (CCK or SST) and the immune immunity gene CD47. Co-expression of two fluorophores was examined by microscopy (Figure 1D). Afterward, cell sorting was performed to select cells with co-expression of the two fluorescent proteins. Based on the results of the sorting, the percentage of DC cells with double positive for miR/CD47-CCK was 43.58%, and the percentage of DC cells with double positive for miR/CD47-SST was 33.74%. (Figure 1E). The double positive cells and miR29b-2 positive cells were collected separately and scaled up for culture. Subsequently, Western blot was used to determine whether the target gene (CCK or SST) and the immune immunity gene CD47 had been successfully delivered to the dendritic cells. It was confirmed by the results that the lentivirus methods used to deliver specific genes to dendritic cells was successful (Figure 1F).

The Characterization of Engineered Exosomes

The dendritic cells successfully transfected with miR-29b-2 with CD47-CCK or CD47-SST lentiviral vectors were amplified and cultured. Exosomes were collected, purified, and concentrated, and their characteristics were analyzed (Table 2). In these exosomes, the protein concentration was between 7083–12,825 μg/mL as determined by a protein quantification reagent. Through qPCR, the effective fragment miR29b-2-5p was quantified, and the concentration of miR29b-2-5p in exosomes transfected with miR29b-2 cells was four times higher than in non-transfected cells. Afterwards, NTA was used to characterize the particles size and concentration. The particle size was between 84.8–100 nm, the particle concentration was between 4.80–7.13×10^{11} particles/mL, and the zeta potential was between (−4.19) and (−6.85) (Table 2). As measured by the NTA, the particle size distributions of the transfected and non-transfected exosomes were highly uniform (Figure 2A). The Western blot was used to confirm the characteristics of exosomes regarding the expression of the transfected protein. All exosomes expressed their characteristic proteins CD81 and HSP70, and exosomes produced by dendritic cells transfected with CD47-CCK or CD47-SST expressed CD47 and target proteins (CCK or SST). These results suggested that these proteins were successfully expressed in exosomes derived from genetic engineering cells (Figure 2B). TEM was used to observe exosome shapes and sizes, and we found that the exosomes had a spherical shape and were similar in size to NTA measurements. (Figure 2C)

Table 2 Protein Content of Exosomes, microRNA Content of Effective Fragments, and Particle Characteristics

Stock (Medium 1/1000x)	Protein	miR29b-2-5p	Particle Size	Particle Conc.	Zeta Potential
	(μg/mL)	(ng/ μL)	(nm)	(Numbers)	(mV)
DC exo	9516.7 ±759.2	53.83±0.15	84.8±3.9	$4.80\times10^{11}\pm9.89\times10^{10}$	−5.68±0.40
DC miR exo	12,825.0±253.7	197.24±0.45	86.1±5.2	$4.94\times10^{11}\pm8.64\times10^{10}$	−4.19±0.95
DC miR / CD47-CCK exo	8216.7±289.8	213.95±0.95	92.6±0.4	$7.13\times10^{11}\pm2.95\times10^{10}$	−5.68 ±1.13
DC miR / CD47-SST exo	7083.3±368.6	202.72±0.55	100.0±4.5	$5.12\times10^{11}\pm7.78\times10^{10}$	−6.85±0.53

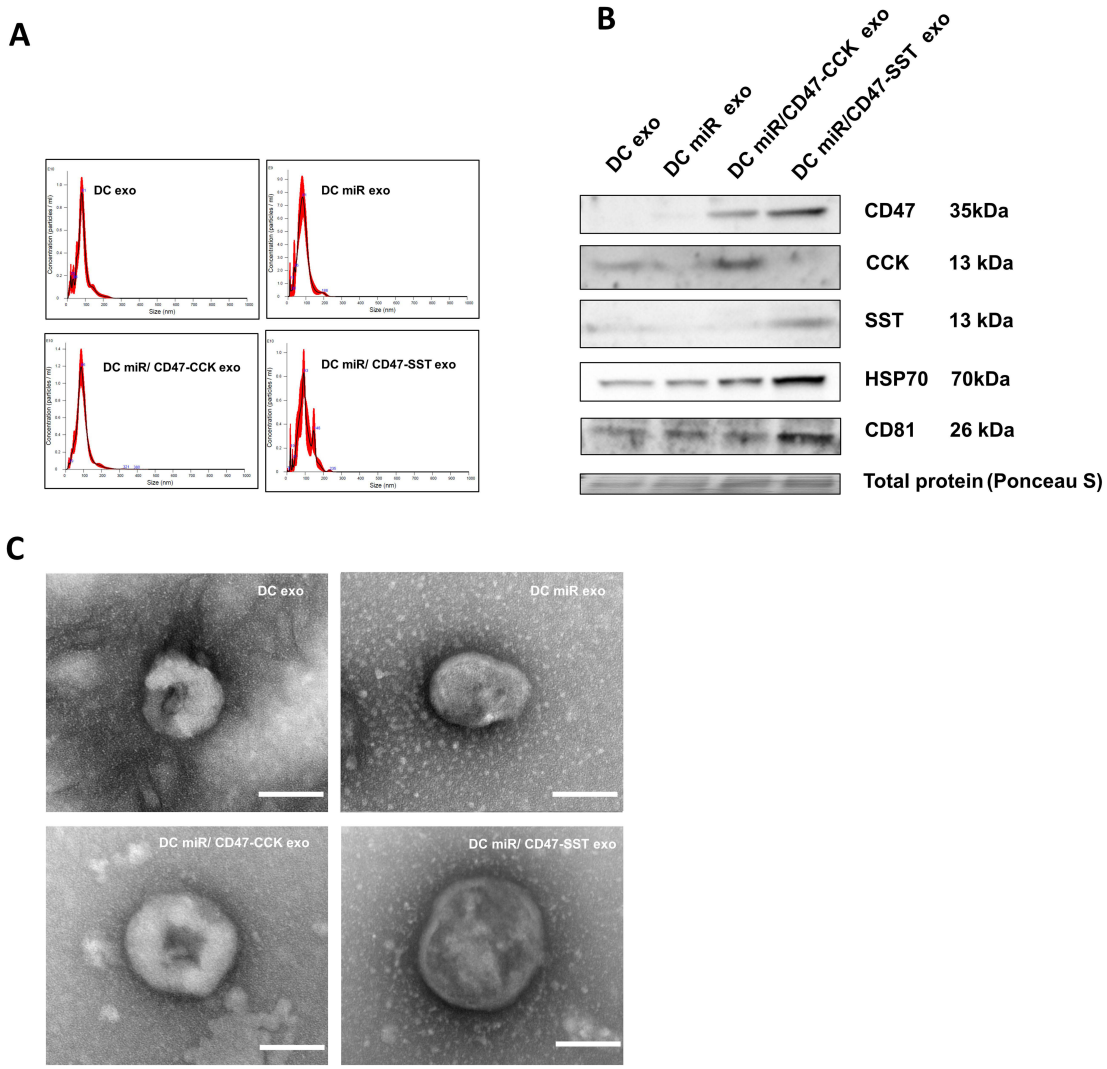

Figure 2 An analysis of exosomes released by dendritic cells transfected with lentiviral vectors containing miR-29b-2 and CD47-CCK /CD47-SST. (**A**) Particle size distribution range. (**B**) Protein expression in engineered exosomes. (**C**) Transmission electron microscopy images of engineered exosomes. (Scale bar represents 100 nm).

Engineered Exosomes Target Cells with Specific Receptors

In order to further verify whether brain neurons could be targeted by exosomes with target genes, we used SH-SY5Y differentiated neural cells and induced them into an AD disease model. Incorporating exosomes into cells was demonstrated by the green fluorescence of DiO-labeled exosomes and the blue fluorescence of the nucleus. In the test cell line SH-SY5Y differentiated into neurons, we found that exosomes containing CCK or SST were more likely to enter the cells with CCKBR and SSTR3 (Figure 3A). When compared to DC exo, there was a 7.3-fold increase in DC miR/CD47-CCK exo and a 4.1-fold increase in DC miR/CD47-SST exo, whereas there was a 1.4-fold increase in DC miR exo (Figure 3B). Western blotting was used to detect receptors related to CCK and SST in this cell model (Figure 3C). These results demonstrated that exosomes expressed CCK and SST had better target capability.

Engineered Exosomes Have Therapeutic Effects in vitro

The therapeutic effects of genetically engineered miR/CD47-CCK and miR/CD47-SST exosomes on disease cell models were studied by adding different groups of exosomes. The study found that, compared to miR exosomes, miR/CD47-CCK exosomes and miR/CD47-SST exosomes containing miR29b-2 significantly inhibited PSEN1 and Aβ1-42 oligomers in diseased SH-SY5Y cells, whereas synthetic miR29b-2-5p had no effects (Figure 3D). DC miR/CD47-CCK exo

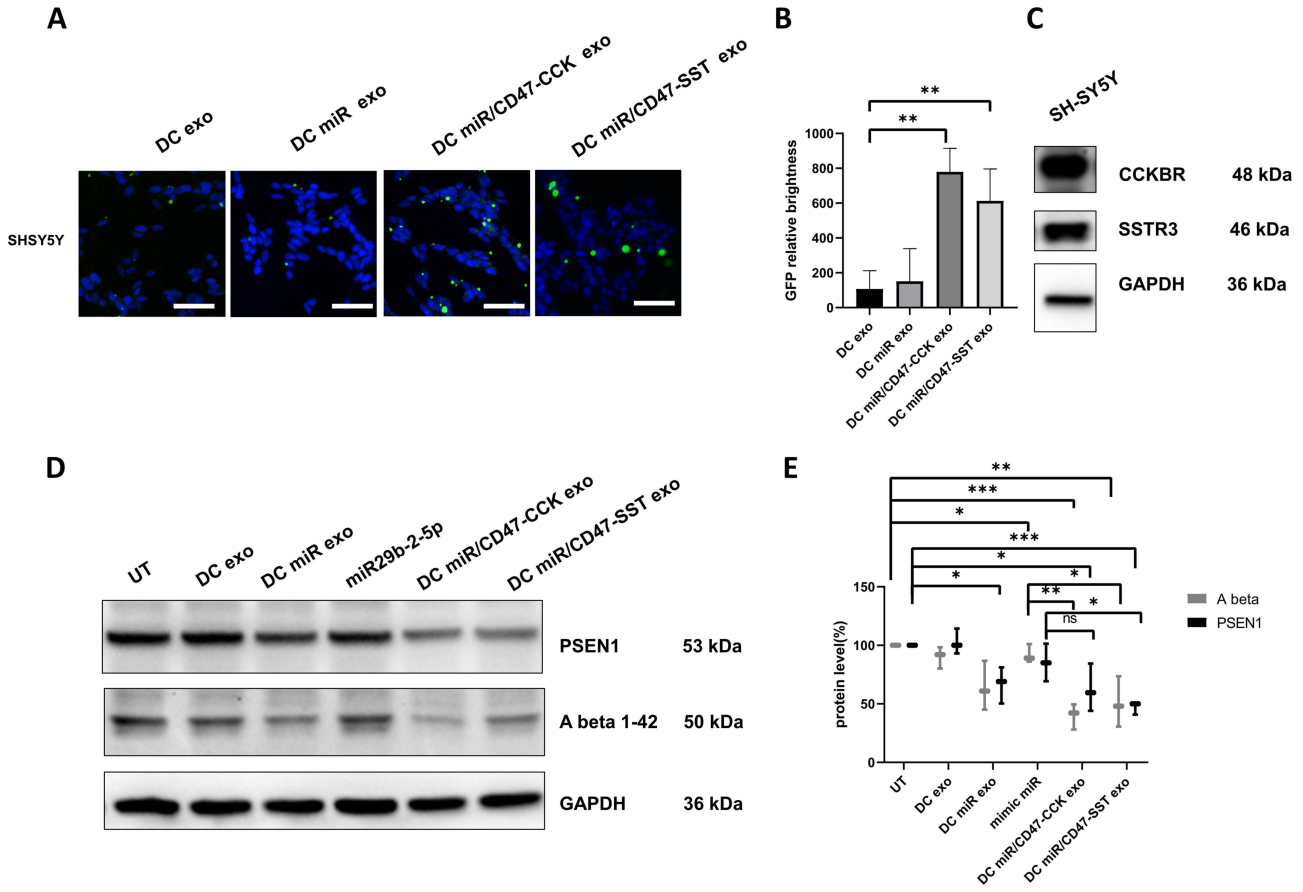

Figure 3 Analysis of engineered exosomes uptake by SH-SY5Y cell line and analysis of engineered exosomes inhibition of disease protein expression. (**A**) DiO-labeled exosomes (green fluorescence) and nuclei of entering cells (blue fluorescence). (Scale bar represents 50 μm). (**B**) Quantification of exosomes entering SHSY5Y cell line. (**C**) The expression of receptor proteins in SH-SY5Y cell line. (**D**) A Western blot analysis of cells treated with different exosome groups in the disease model SH-SY5Y. (**E**) Quantification of disease protein levels in SH-SY5Y cells. *p < 0.05, **p < 0.01, ***p < 0.001.

and DC miR/CD47-SST exo inhibited 60.1% and 49.3% of A beta, respectively, both of which were significantly different from those inhibited by DC miR exo (35.8%) and mimic miR29-2-5p (8%). However, DC miR/CD47-CCK exo, DC miR/CD47-SST exo, DC miR exo, and mimic miR29-2-5p inhibited 37.4%, 52.8%, 33.2%, and 14.8% of PSEN1, respectively. Thus, DC miR/CD47-SST exo had the greatest inhibitory activity (Figure 3E).

Engineered Exosomes are Effective as a Therapeutic Agent in vivo

As a further measure of the effectiveness of engineered exosomes in vivo, we also administered different groups of engineered exosomes intravenously to 3xTg-AD mice, an animal model of AD. The mice were sacrificed three days following the treatment, and their brains were removed and divided into three parts: the hippocampus, the cortex, and other brain areas. Following the extraction of proteins, Western blot analysis of the proteins was performed (Figure 4A). According to the experimental results, miR/CD47-SST exosomes significantly inhibited the expression of PSEN1 protein in the mouse hippocampus (48.3% of the data in untreated mice) and cortex (22.3% of the data in untreated mice) when compared with the DC control group. It also inhibited the expression of the protein Aβ1-42 Oligomer in hippocampus (45.6% of the data in untreated mice) and cortex (63.6% of the data in untreated mice) (Figure 4B and C). However, miR/CD47-CCK exosomes had a significant inhibitory effect only on Aβ1-42 Oligomer in cortex (42.3% of the data in untreated mice). As well, IHC was used to examine the Aβ1-42 Oligomer in the mouse hippocampus. Results showed that the miR/CD47-SST exosome group had the least amount of amyloid accumulation compared to the DC control group (Figure 4D). Thus, miR/CD47-SST exosomes were selected as a more effective therapeutic option. In light of this, the purpose of this study was to observe this particular group of DC miR/CD47-SST exosomes.

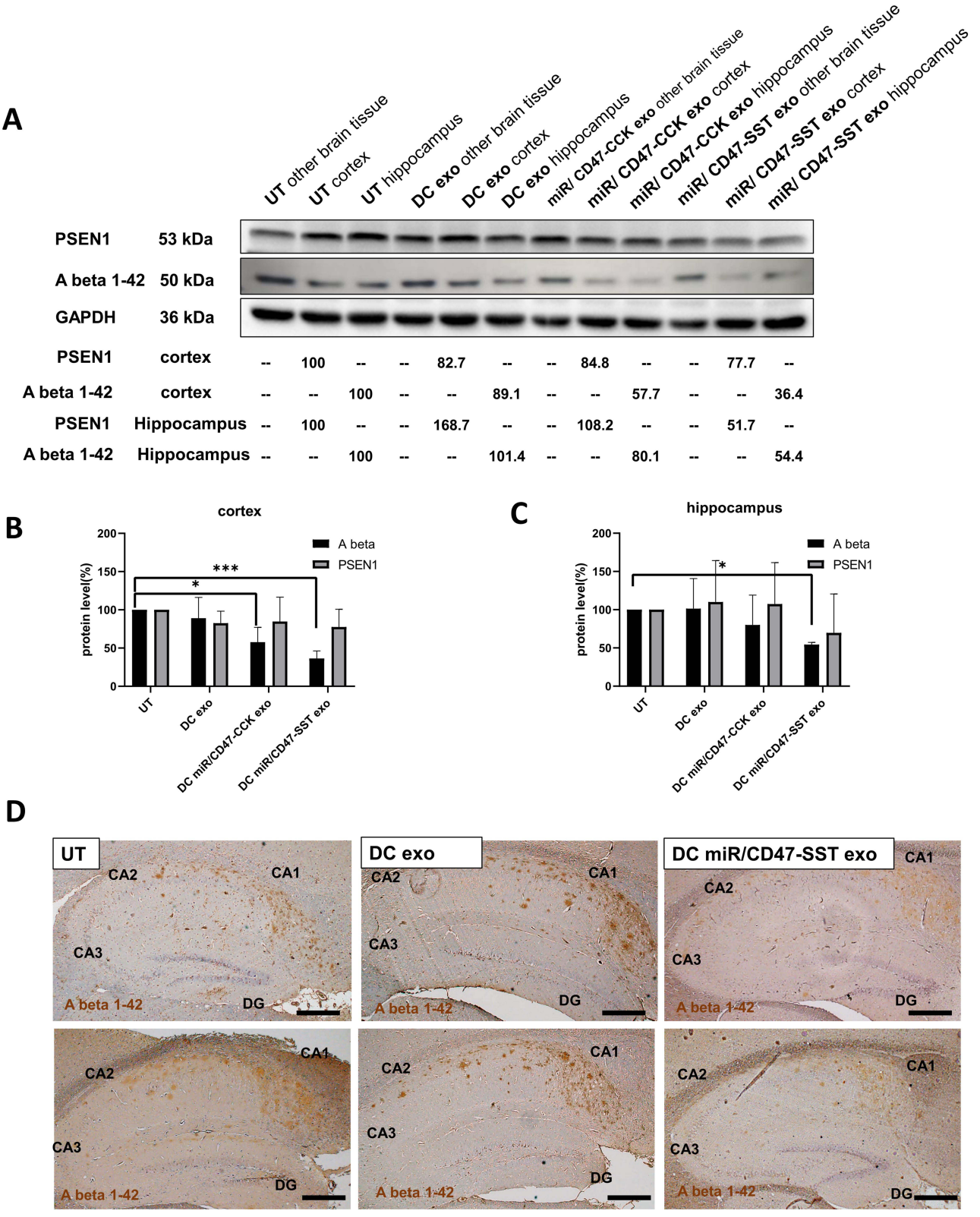

Figure 4 Engineered exosomes inhibit disease proteins in 3xTg-AD mice. (**A**–**C**) The Western blot and quantitative results of the brain tissue from 3xTg-AD mice were analyzed after three days of treatment. * $p < 0.05$ *** $p < 0.001$. (**D**) The Aβ 1–42 oligomers protein content of the 3xTg-AD mouse hippocampus was examined with IHC. (Scale bar represents 200 μm).

The Hippocampus of the Brain Can Be Targeted by Engineered Exosomes in vivo

Initially, we examined the systemic distribution of engineered exosomes in vivo by IVIS as described in Materials and Methods section. As shown in the experimental results, the DC miR/CD47-SST exosomes were distributed more in the brain (21.3-fold of the data in untreated mice) when compared to the DC control exosomes (16.6-fold of the data in untreated mice) (Figure 5A and B).

In order to demonstrate our engineered exosomes can be more effectively delivered via intravenous injection to the hippocampal region, we used IHC staining to detect if exogenous proteins (CD47, SST, and the exosome marker CD63) of engineered exosomes expressed in the hippocampus. The expression of CD47 and SST was not observed in the stains of the untreated group. The expression of CD63 was seen in the stains of DC exosome while CD47 and SST was not

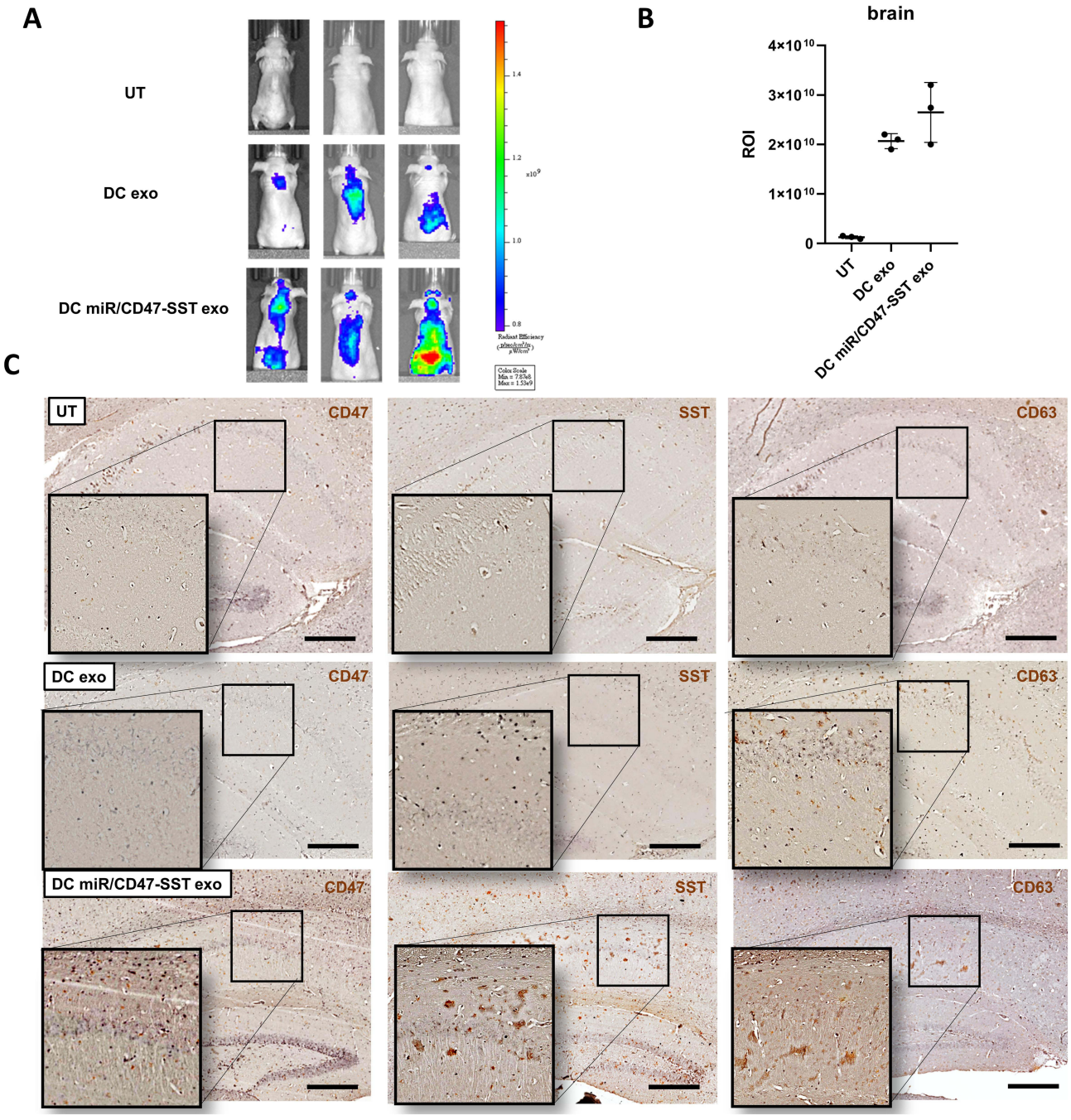

Figure 5 Engineered exosomes delivered intravenously to mice's brains. (**A**) Nude mice were injected intravenously with different groups of exosomes for 24 hours and their IVIS results were analyzed in vivo. (**B**) An analysis of the quantitative results of IVIS experiments on brain brightness. (**C**) The exosomal protein CD63 with CD47 and SST in the hippocampal region. (Scale bar represents 200 μm).

present, suggesting DC exosomes were able to reach the hippocampus. We observed the expression of CD47, SST, and CD63 in the IHC stains of the DC miR/CD47-SST exosomes group, indicating that the engineered exosomes had effectively reached the hippocampus. Moreover, the CD63 signal of the DC exosome group and that of the DC miR/CD47-SST group seemed to suggest more engineered exosomes had reached the hippocampus (Figure 5C).

Targeting of SST Exosomes is Directly Related to the SST Receptor

Through counter-evidence, we demonstrated that silencing SST receptor 3 in the SH-SY5Y cell line affected the ability of miR/CD47-SST exosomes to enter cells. To begin, we tested the dose of si-SSTR3 to inhibit SST receptor 3 and found that 3 micrograms of si-SSTR3 in a 24-well plate inhibited 83.6% of SST receptor 3, but no significant inhibitory effect was observed when the concentration was increased (Figure 6A and B). Accordingly, we chose this concentration for

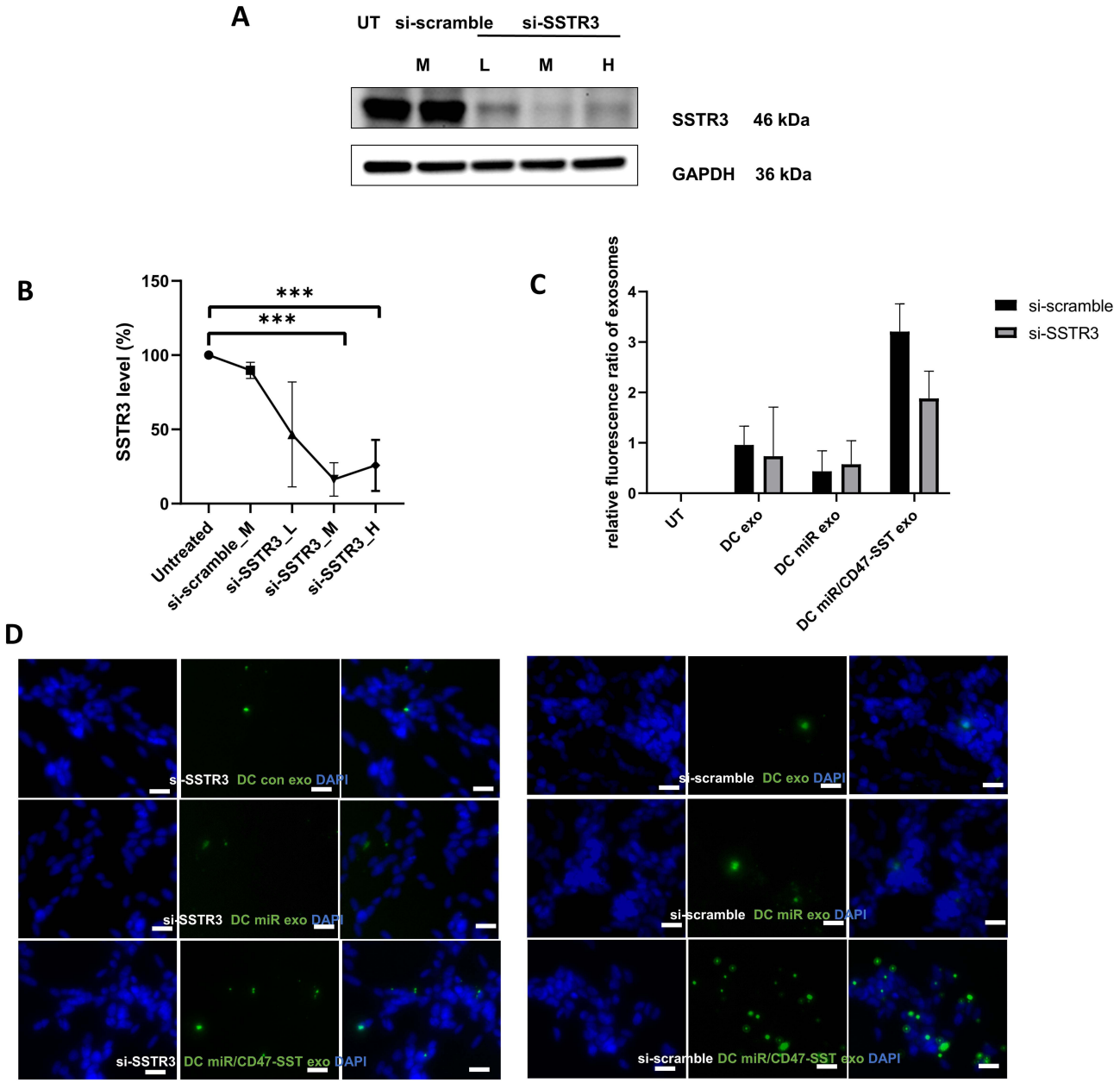

Figure 6 The uptake of SST target exosomes in knockdown SST receptor cells. (**A**) Silence RNA inhibition of SST receptor 3 in SH-SY5Y cells. (**B**) An analysis of the quantitative results of silence RNA inhibition of the SST receptor 3 in SH-SY5Y cells. (**C**) Quantitative analysis of the entrance of exosomes into SH-SY5Y cells (***$p < 0.001$). (**D**) As the SST receptor 3 was inhibited by silence RNA, the number of CD47-SST exosomes entering SH-SY5Y cells decreased. (Scale bar represents 20 μm).

later experiments. We then separately transfected si-scramble and si-SSTR3 into the SH-SY5Y cell line. Subsequently, different groups of exosomes with Dio green fluorescence were added. After 12 hours, wash the cells and observe exosomes entering the cell under a fluorescence microscope. According to the results, the amount of miR/CD47-SST exosome entering the cells in the group that was treated with si-scramble (3.2-fold of the data in DC exosome treated with si-scramble) was higher than the amount entering the cells when si-SSTR3 was used to inhibit the receptor was lower (1.9-fold of the data in DC exosome treated with si-scramble) (Figure 6C and D). This indicates that miR/CD47-SST exosome entry into cells was directly related to the number of receptors on the cells.

Discussion

AD (AD) is the most common form of dementia.[38] The two main pathological features of AD are the extracellular deposition and accumulation of amyloid Aβ and neurofibrillary tangles containing hyperphosphorylated tau protein in neurons.[39] The main factor involved in the formation of Aβ peptide is the simultaneous cleavage of toxic Aβ peptide fragments by β-secretase and γ-secretase. γ-Secretase is a transmembrane protein complex that contains presenilin, nicastrin, Aph-1, and Pen-2. More than 140 substrates are cleaved by γ-secretase, including APP and Notch. In particular, various amyloid peptides are produced by sequential digestion of the carboxyl-terminal fragment of APP (APP-C99) by γ-secretase.[40] The accumulation of Aβ peptides (eg, Aβ42 and Aβ43) leads to the formation of amyloid plaques in the brain, a hallmark of AD.[41] Therefore, γ-secretase is considered to be an attractive treatment target for AD.

Mutations to PSEN1 on γ-secretase have been shown to affect APP processing and Aβ peptide production, and to inhibit Notch1 cleavage and Notch signaling. Therefore, inhibitors with specific active site specificities have been used to study the recognition of γ-secretase substrates.[42] In addition, abnormal cleavage of Notch by γ-secretase was associated with various types of cancer.[43] The use of γ-secretase inhibitors is also used to block Notch activity and prevent the cleavage of Notch on the cell surface, which can also be used as a method of treating cancer.[43,44] However, γ-secretase inhibitors (GSIs) have been shown in clinical trials to cause side effects due to inhibition of Notch signaling.[45] Understanding the mechanism by which γ-secretase recognizes substrates may help the development of substrate-specific inhibitors.[46] However, some studies have found that Notch signaling may not be critical to the pathogenesis of AD, since inhibiting the mutant PSEN1 protein does not affect the Notch pathway. The involvement of serine 169 may serve as a potential target for deriving new γ-secretase regulatory targets without affecting Notch1 cleavage to treat AD.[47] According to our previous study, miR29b-2-5p was able to reduce the levels of PSEN1, a protein associated with γ-secretase.[2] Accordingly, miR29b-2-5p shows promise as a therapeutic agent for AD.

As a natural carrier for intracellular biomolecules, exosomes have the potential to deliver proteins, mRNA, and miRNA to desired cells, thereby regulating their physiological or pathological functions.[48] In addition, exosomes can be loaded with exogenous siRNA through electroporation as well as bioengineered to carry the hippocampal-targeting ligand RVG.[49] SiRNA is considered to be an exogenous double-stranded RNA that is absorbed by cells. Therefore, it enters through vectors such as viruses. While miRNA is a single-stranded RNA, it originates from endogenous non-coding RNAs that are found in introns of larger RNA molecules. In animals, siRNA frequently binds well to its target mRNA. It is a perfect match with the sequence. Since miRNAs are not perfectly paired, they may inhibit the translation of many different mRNA sequences. When the mRNA changes and binds to a specific ribosome site, translation would take place. By cleaving mRNA rather than inhibiting its translation, miRNA induces mRNA degradation. SiRNA and miRNA are both capable of playing a role in epigenetics through RNA-induced transcriptional silencing (RITS).[50] We use miRNA as the oligonucleotide drugs used in this study. Through the characteristics of exosomes crossing physiological barriers and reducing immunogenicity, we further prove that exosomes carrying miR29b-2 are more effective in inhibiting PSEN1 than naked miR29b-2 in the AD cells model (Figure 3D and E).

In our preliminary research on the small molecule drug n-BP in treating AD, we determined that miR-29b-2-5p regulated PSEN1 and reduced the production of amyloid proteins.[2] Furthermore, a previous study had indicated that engineered exosomes carrying miR29b can reduced the pathological effects of Aβ peptide in AD rat models and effectively treat cognitive impairment in AD rats.[51] The exosomes carrying miR-29b-1 or miR-29b-2 inhibited BACE1. The common fragment of miR-29b-1 or miR-29b-2 was miR-29b-3p. In our study, we found that HEK293 cells transfected with miR-29b-2 produced exosomes that contained higher levels of miR-29b-2-5p than miR-29b-3p (Figure S1). Thus, we examined the effects of miR-29b-2, the upstream fragment of miR-29b-2-5p on PSEN1 in this study.

In order to ensure more accurate delivery of the target ligand to the treatment site, we designed genetic engineering techniques to deliver the ligand to the membrane of exosomes. It has been reported that SST receptors are highly expressed in the hippocampus.[29] Consequently, we designed miR(miR29b-2)/CD47-SST exosomes for target to cells or animals through SST receptors.

The full name of the 3xTg-AD mouse is B6;129-Tg (APPSwe, tauP301L)1Lfa Psen1^{tm1Mpm} /Mmjax, which carries the mutation PS1M146V associated with familial AD in humans. The mice were viable, fertile, and did not exhibit any physical or behavioral abnormalities. The mRNA of the target mutant allele behaved normally in Northern blot analysis and RT-PCR.[52] The overexpression of the transgene appears to be restricted to areas associated with AD, such as the hippocampus and cerebral cortex. Cells expressing the mutant protein PS1M146V exhibit disrupted calcium homeostasis in neurons. This model is therefore suitable for examining the inhibition of PSEN1. According to the results, exosomes containing CD47-SST exhibited higher cellular uptake in both cell and animal models of AD (Figures 3A and 5B). A knockdown of SST receptor 3 in SH-SY5Y cells significantly reduced the uptake of miR/CD47-SST exosomes (Figure 6D). Due to its ability to target cells with SST receptors or an animal's hippocampus, SST can target cells with specific SST receptors. By expressing CD47 on the membrane, we found that SST could be transported within exosomes. Exosomes we produced were also confirmed to contain CD47 (Figure 2B). In mice, CD47-SST exosomes retained well and delivered to specific sites after intravenous injection (Figure 5A). Further, we used IHC to stain CD63 on exosomes as well as miR/CD47-SST exosomes containing CD47 and SST. A significant increase in CD63, SST, and CD47 was observed in mouse subjects injected with miR/CD47-SST exosomes through the tail vein (Figure 5C). Three antibodies appear in the same location, indicating that the proteins may come from exogenous exosomes. IHC staining confirmed that the CD47, SST, and CD63 proteins were located on exosome surfaces. And the DC miR/CD47-SST exosomes successfully reached the hippocampus via intravenous injection (Figure 5C). It is because that the brain shows a considerable amount of SST receptor expression, especially in the hippocampal region.[29,53,54] However, in addition to brain, we also observed the IVIS expression of engineered exosomes in other areas such as gastrointestinal tract. Taniyama et al, reported the presence of SST receptors in the central nervous system and other abdominal 5 organs.[55] Considering the broad distribution of these engineered exosomes, a proper design of transplantation strategy (such as nasal delivery) will be required for their clinical application. The toxic effect of these transplanted engineered exosomes was also assessed by tissue H&E staining. No significant abnormal findings were observed in the treatment groups as compared with those in the control groups. (Figure S2).

Conclusion

Based on the findings of this study, a cell platform capable of producing engineered exosomes was successfully developed. In order to produce exosomes with the designed functions, we transfected microRNA29b-2, immunity protein gene CD47, and target protein gene CCK or SST into immature dendritic cells and confirmed that established cell models could express these microRNAs or target proteins. Exosomes targeting SST inhibit PSEN1 more effectively than exosomes without targeting ligand or modified CCK. The result of this study was the development of engineered exosomes model that could prove useful in treating AD. In the future, this technique may be applied to carry other microRNAs or proteins for the production of new engineered exosomes.

Abbreviations

exo, exosome; CCK, cholecystokinin; SST, somatostatin; PSEN1, presenilin 1; miR, microRNA-29b-2; AD, Alzheimer's disease; Aβ, beta-amyloid or β-amyloid; ASO, antisense oligonucleotide; siRNA, small interfering RNA; miRNA, microRNA; mRNA, message RNA; DC, dendritic cells; ECM, extracellular matrix; APP, amyloid precursor protein; BACE1, β-secretase 1; BIM, Bcl-2-like protein 11; NAV3, Neuron Navigator 3; IHC, Immunohistochemistry.

Acknowledgments

We express our gratitude to Professor Yu-Ru Kou for his valuable suggestions regarding the preparation of this manuscript. We would like to acknowledge Ms. Ching-Tsz Lin for sharing her technical expertise in plasmid construction. We would like to thank the Electron Microscopy Laboratory of Tzu Chi University for their assistance in conducting the TEM experiment. Finally, we are grateful for the support of The Bioinnovation Center, Buddhist Tzu Chi Medical Foundation, Hualien, Taiwan.

Funding

This work was supported by National Science and Technology Council, Taiwan (MOST-107-2221-E-259-010- MY3, MOST-110-2221-E-259-002, MOST-111-2320-B-303 −002 -MY3).

Disclosure

The authors report no conflicts of interest in this work.

References

1. World Health Organization. Dementia. Available from: https://www.who.int/news-room/fact-sheets/detail/dementia. Accessed March 15, 2023.
2. Wuli W, Lin SZ, Chen SP, et al. Targeting PSEN1 by lnc-CYP3A43-2/miR-29b-2-5p to reduce beta amyloid plaque formation and improve cognition function. *Int J Mol Sci*. 2022;23(18). doi:10.3390/ijms231810554
3. Reitz C, Rogaeva E, Beecham GW. Late-onset vs nonmendelian early-onset Alzheimer disease: a distinction without a difference? *Neurol Genet*. 2020;6(5):e512. doi:10.1212/NXG.0000000000000512
4. Li YS, Yang ZH, Zhang Y, et al. Two novel mutations and a de novo mutation in PSEN1 in early-onset alzheimer's disease. *Aging Dis*. 2019;10(4):908–914. doi:10.14336/AD.2018.1109
5. Lanoiselee HM, Nicolas G, Wallon D, et al. APP, PSEN1, and PSEN2 mutations in early-onset Alzheimer disease: a genetic screening study of familial and sporadic cases. *PLoS Med*. 2017;14(3):e1002270. doi:10.1371/journal.pmed.1002270
6. Wragg M, Hutton M, Talbot C, Goate A. Genetic association between intronic polymorphism in presenilin-1 gene and late-onset Alzheimer's disease. Alzheimer's Disease Collaborative Group. *Lancet*. 1996;347(9000):509–512. doi:10.1016/S0140-6736(96)91140-X
7. Crooke ST. Molecular Mechanisms of Antisense Oligonucleotides. *Nucleic Acid Ther*. 2017;27(2):70–77. doi:10.1089/nat.2016.0656
8. Dexheimer PJ, Cochella L. MicroRNAs: from mechanism to organism. *Front Cell Dev Biol*. 2020;8:409. doi:10.3389/fcell.2020.00409
9. Bartel DP. Metazoan MicroRNAs. *Cell*. 2018;173(1):20–51. doi:10.1016/j.cell.2018.03.006
10. Amakiri N, Kubosumi A, Tran J, Reddy PH. Amyloid Beta and MicroRNAs in Alzheimer's Disease. *Front Neurosci*. 2019;13:430. doi:10.3389/fnins.2019.00430
11. Fransquet PD, Ryan J. Micro RNA as a potential blood-based epigenetic biomarker for Alzheimer's disease. *Clin Biochem*. 2018;58:5–14. doi:10.1016/j.clinbiochem.2018.05.020
12. Kiko T, Nakagawa K, Tsuduki T, Furukawa K, Arai H, Miyazawa T. MicroRNAs in plasma and cerebrospinal fluid as potential markers for Alzheimer's disease. *J Alzheimers Dis*. 2014;39(2):253–259. doi:10.3233/JAD-130932
13. Lin EY, Chen YS, Li YS, et al. Liposome consolidated with cyclodextrin provides prolonged drug retention resulting in increased drug bioavailability in brain. *Int J Mol Sci*. 2020;21(12):1.
14. Goldie BJ, Dun MD, Lin M, et al. Activity-associated miRNA are packaged in Map1b-enriched exosomes released from depolarized neurons. *Nucleic Acids Res*. 2014;42(14):9195–9208. doi:10.1093/nar/gku594
15. Garcia-Martin R, Wang G, Brandao BB, et al. MicroRNA sequence codes for small extracellular vesicle release and cellular retention. *Nature*. 2022;601:446–451. doi:10.1038/s41586-021-04234-3
16. Valadi H, Ekstrom K, Bossios A, Sjostrand M, Lee JJ, Lotvall JO. Exosome-mediated transfer of mRNAs and microRNAs is a novel mechanism of genetic exchange between cells. *Nat Cell Biol*. 2007;9(6):654–659. doi:10.1038/ncb1596
17. Zhao L, Jiang X, Shi J, et al. Exosomes derived from bone marrow mesenchymal stem cells overexpressing microRNA-25 protect spinal cords against transient ischemia. *J Thorac Cardiovasc Surg*. 2019;157(2):508–517. doi:10.1016/j.jtcvs.2018.07.095
18. Pu L, Kong X, Li H, He X. Exosomes released from mesenchymal stem cells overexpressing microRNA-30e ameliorate heart failure in rats with myocardial infarction. *Am J Transl Res*. 2021;13(5):4007–4025.
19. Jin Z, Ren J, Qi S. Human bone mesenchymal stem cells-derived exosomes overexpressing microRNA-26a-5p alleviate osteoarthritis via down-regulation of PTGS2. *Int Immunopharmacol*. 2020;78:105946. doi:10.1016/j.intimp.2019.105946
20. Li Q, Wang H, Peng H, Huyan T, Cacalano NA. Exosomes: versatile nano mediators of immune regulation. *Cancers*. 2019;11:1.
21. Yin W, Ouyang S, Li Y, Xiao B, Yang H. Immature dendritic cell-derived exosomes: a promise subcellular vaccine for autoimmunity. *Inflammation*. 2013;36(1):232–240. doi:10.1007/s10753-012-9539-1
22. Yang X, Meng S, Jiang H, Zhu C, Wu W. Exosomes derived from immature bone marrow dendritic cells induce tolerogenicity of intestinal transplantation in rats. *J Surg Res*. 2011;171(2):826–832. doi:10.1016/j.jss.2010.05.021
23. Jan AT, Rahman S, Badierah R, et al. Expedition into exosome biology: a perspective of progress from discovery to therapeutic development. *Cancers*. 2021;13(5):1157. doi:10.3390/cancers13051157
24. van de Water FM, Boerman OC, Wouterse AC, Peters JG, Russel FG, Masereeuw R. Intravenously administered short interfering RNA accumulates in the kidney and selectively suppresses gene function in renal proximal tubules. *Drug Metab Disposit*. 2006;34(8):1393–1397. doi:10.1124/dmd.106.009555
25. Del Valle J, Duran-Vilaregut J, Manich G, et al. Early amyloid accumulation in the hippocampus of SAMP8 mice. *J Alzheimers Dis*. 2010;19(4):1303–1315. doi:10.3233/JAD-2010-1321
26. Pearson-Leary J, McNay EC. Intrahippocampal administration of amyloid-β(1-42) oligomers acutely impairs spatial working memory, insulin signaling, and hippocampal metabolism. *J Alzheimers Dis*. 2012;30(2):413–422. doi:10.3233/jad-2012-112192
27. Rehfeld JF. Cholecystokinin—From local gut hormone to ubiquitous messenger. *Front Endocrinol (Lausanne)*. 2017;8:47. doi:10.3389/fendo.2017.00047
28. Gastambide F, Lepousez G, Viollet C, Loudes C, Epelbaum J, Guillou JL. Cooperation between hippocampal somatostatin receptor subtypes 4 and 2: functional relevance in interactive memory systems. *Hippocampus*. 2010;20(6):745–757. doi:10.1002/hipo.20680
29. Nakamura NH, Akiyama K, Naito T. Quantitative gene-expression analysis of the ligand-receptor system for classical neurotransmitters and neuropeptides in hippocampal CA1, CA3, and dentate gyrus. *Hippocampus*. 2011;21(11):1228–1239. doi:10.1002/hipo.20830

30. Chauhan S, Danielson S, Clements V, Edwards N, Ostrand-Rosenberg S, Fenselau C. Surface glycoproteins of exosomes shed by myeloid-derived suppressor cells contribute to function. *J Proteome Res*. 2017;16(1):238–246. doi:10.1021/acs.jproteome.6b00811
31. Yang Z, Shi J, Xie J, et al. Author Correction: large-scale generation of functional mRNA-encapsulating exosomes via cellular nanoporation. *Nat Biomed Eng*. 2021;5(8):944–945. doi:10.1038/s41551-021-00725-w
32. Zhang W, Huang Q, Xiao W, et al. Advances in Anti-Tumor Treatments Targeting the CD47/SIRPalpha Axis. *Front Immunol*. 2020;11:18. doi:10.3389/fimmu.2020.00018
33. Kamerkar S, LeBleu VS, Sugimoto H, et al. Exosomes facilitate therapeutic targeting of oncogenic KRAS in pancreatic cancer. *Nature*. 2017;546:498–503. doi:10.1038/nature22341
34. Kaur S, Singh SP, Elkahloun AG, Wu W, Abu-Asab MS, Roberts DD. CD47-dependent immunomodulatory and angiogenic activities of extracellular vesicles produced by T cells. *Matrix Biol*. 2014;37:49–59. doi:10.1016/j.matbio.2014.05.007
35. Vestad B, Llorente A, Neurauter A, et al. Size and concentration analyses of extracellular vesicles by nanoparticle tracking analysis: a variation study. *J Extracell Vesicles*. 2017;6(1):1344087. doi:10.1080/20013078.2017.1344087
36. Midekessa G, Godakumara K, Ord J, et al. Zeta potential of extracellular vesicles: toward understanding the attributes that determine colloidal stability. *ACS Omega*. 2020;5(27):16701–16710. doi:10.1021/acsomega.0c01582
37. de Medeiros LM, De Bastiani MA, Rico EP, et al. Cholinergic differentiation of human neuroblastoma SH-SY5Y cell line and its potential use as an in vitro model for alzheimer's disease studies. *Mol Neurobiol*. 2019;56(11):7355–7367. doi:10.1007/s12035-019-1605-3
38. Mehta RI, Schneider JA. Neuropathology of the Common Forms of Dementia. *Clin Geriatr Med*. 2023;39(1):91–107. doi:10.1016/j.cger.2022.07.005
39. Sengoku R. Aging and Alzheimer's disease pathology. *Neuropathology*. 2020;40(1):22–29. doi:10.1111/neup.12626
40. Takami M, Nagashima Y, Sano Y, et al. gamma-Secretase: successive tripeptide and tetrapeptide release from the transmembrane domain of beta-carboxyl terminal fragment. *J Neurosci*. 2009;29(41):13042–13052. doi:10.1523/JNEUROSCI.2362-09.2009
41. Hardy J. The discovery of Alzheimer-causing mutations in the APP gene and the formulation of the "amyloid cascade hypothesis". *FEBS J*. 2017;284(7):1040–1044. doi:10.1111/febs.14004
42. Johnson DS, Li YM, Pettersson M, St George-Hyslop PH. Structural and chemical biology of presenilin complexes. *Cold Spring Harb Perspect Med*. 2017;7(12):a024067. doi:10.1101/cshperspect.a024067
43. Medoro A, Bartollino S, Mignogna D, et al. Complexity and selectivity of gamma-secretase cleavage on multiple substrates: consequences in alzheimer's disease and cancer. *J Alzheimers Dis*. 2018;61(1):1–15. doi:10.3233/JAD-170628
44. Wang D, Xu J, Liu B, et al. IL6 blockade potentiates the anti-tumor effects of gamma-secretase inhibitors in Notch3-expressing breast cancer. *Cell Death Differ*. 2018;25(2):330–339. doi:10.1038/cdd.2017.162
45. Nguyen V, Hawkins C, Bergeron C, et al. Loss of nicastrin elicits an apoptotic phenotype in mouse embryos. *Brain Res*. 2006;1086(1):76–84. doi:10.1016/j.brainres.2006.02.122
46. Yang G, Zhou R, Zhou Q, et al. Structural basis of Notch recognition by human gamma-secretase. *Nature*. 2019;565:192–197. doi:10.1038/s41586-018-0813-8
47. Zhang S, Cai F, Wu Y, et al. A presenilin-1 mutation causes Alzheimer disease without affecting Notch signaling. *Mol Psychiatry*. 2020;25(3):603–613. doi:10.1038/s41380-018-0101-x
48. Zhang Y, Liu Y, Liu H, Tang WH. Exosomes: biogenesis, biologic function and clinical potential. *Cell Biosci*. 2019;9(1):19. doi:10.1186/s13578-019-0282-2
49. Alvarez-Erviti L, Seow Y, Yin H, Betts C, Lakhal S, Wood MJ. Delivery of siRNA to the mouse brain by systemic injection of targeted exosomes. *Nat Biotechnol*. 2011;29(4):341–345. doi:10.1038/nbt.1807
50. Lam JK, Chow MY, Zhang Y, Leung SW. siRNA Versus miRNA as therapeutics for gene silencing. *Mol Ther Nucleic Acids*. 2015;4(9):e252. doi:10.1038/mtna.2015.23
51. Jahangard Y, Monfared H, Moradi A, Zare M, Mirnajafi-Zadeh J, Mowla SJ. Therapeutic effects of transplanted exosomes Containing miR-29b to a rat model of alzheimer's disease. *Front Neurosci*. 2020;14:564. doi:10.3389/fnins.2020.00564
52. Guo Q, Fu W, Sopher BL, et al. Increased vulnerability of hippocampal neurons to excitotoxic necrosis in presenilin-1 mutant knock-in mice. *Nat Med*. 1999;5(1):101–106. doi:10.1038/4789
53. Szentes N, Tekus V, Mohos V, Borbely E, Helyes Z. Exploratory and locomotor activity, learning and memory functions in somatostatin receptor subtype 4 gene-deficient mice in relation to aging and sex. *Geroscience*. 2019;41(5):631–641. doi:10.1007/s11357-019-00059-1
54. Raulf F, Perez J, Hoyer D, Bruns C. Differential expression of five somatostatin receptor subtypes, SSTR1-5, in the CNS and peripheral tissue. *Digestion*. 1994;55(3):46–53. doi:10.1159/000201201
55. Taniyama Y, Suzuki T, Mikami Y, Moriya T, Satomi S, Sasano H. Systemic distribution of somatostatin receptor subtypes in human: an immunohistochemical study. *Endocr J*. 2005;52(5):605–611. doi:10.1507/endocrj.52.605